Interferometric focusing of guide-stars for direct wavefront sensing

Xiaodong Tao*[a], Ziah Dean[b], Christopher Chien[c], Oscar Azucena[a], Joel Kubby[a]

[a]Department of Electrical Engineering, University of California, Santa Cruz, 1156 High St., Santa Cruz, CA 95064, USA; [b]Department of Biophysics, University of Michigan, 930 N. University Ave., Ann Arbor, MI 48109, USA; [c]Department of Biology, University of California, Santa Cruz, 1156 High St., Santa Cruz, CA 95064, USA

ABSTRACT

Optical microscopy allows noninvasive imaging of biological tissues at a subcellular level. However, the optimal performance of the microscope is hard to achieve because of aberrations induced from tissues. The shallow penetration depth and degraded resolution provide a limited degree of information for biologists. In order to compensate for aberrations, adaptive optics with direct wavefront sensing, where guide-stars are used for wavefront measurement, has been applied in microscopy. The scattering effect limits the intensity of a guide-star and hence reduces the signal to noise ratio of the wavefront measurement. In this paper, we propose to use interferometric focusing of excitation light onto a guide-star embedded deeply in tissue to increase its fluorescence intensity, thus overcoming the signal loss caused by scattering. With interferometric focusing of light, we increase the signal to noise ratio of the laser guide-star through scattering tissue by more than two times as well as potentially extending the thickness of tissue that can be corrected using AO microscopy.

Keywords: Adaptive Optics, Interferometic Focusing, Scattering, Guide-stars

1. INTRODUCTION

Optical microscopy has become an important tool for biological research and continues to open new avenues in its capabilities. However, the penetration depth for optical imaging is still limited. As light passes through biological tissue it can be absorbed, refracted and scattered, limiting the resolution and depth of optical imaging in biological tissues. Overcoming these challenges will significantly extend the imaging depth while maintaining subcelluar resolution. Adaptive optics using direct wavefront sensing has been applied to live deep-tissue imaging to correct for aberrations caused by refraction, enabling near diffraction limited imaging through thick tissues [1,2]. While the wavefront measurement depends on the emission light from the guide-star, the scattering effect will not only limit the amount of photons delivered to the guide-star, but also increase the background noise from neighboring guide-stars. Both of these effects reduce the signal to noise ratio (SNR) for wavefront measurements.

Scattering is caused by inhomogeneities in biological tissues. It has been shown that the majority of light scattering from a cell is due to the nucleus and smaller organelles such as mitochondria [3]. The elastic scattering is an order of magnitude or more than the absorption. Although scattering is entirely random, it is a deterministic and time reversible process. The optical phase conjugation (OPC) method has been successfully applied to measure the phase and amplitude of the scattered light field, retrace its trajectory through the scattering medium and recover its original input light field [4]. To measure the light field coming from the observed area, OPC needs coherent light from the area of interest. In a more recent study, ultrasonically encoded focusing has been applied to generate a guide-star as a coherent point source for phase measurement [5]. Instead of direct measurement of the optical field, another method, called inteferometric focusing, is used to estimate the optimal phase of the scattering light field by modulating the phase of illumination light while analyzing the variation of emission light from the target [6]. By measuring the phase of scattered light from the point source in the sample one can match the scattering behavior of the turbid material and as a result allow constructive interference to occur, thereby increasing intensity at the point source. In conventional focusing the paths of light rays are

*taoxd@soe.ucsc.edu;

MEMS Adaptive Optics VII, edited by Scot S. Olivier, Thomas G. Bifano, Joel Kubby, Proc. of SPIE
Vol. 8617, 86170E · © 2013 SPIE · CCC code: 0277-786X/13/$18 · doi: 10.1117/12.2006118

determined by Fermat's principle of least time; light will take a path between two points that minimizes the travel time. Interferometric focusing uses the coherent properties of light to cause constructive interference at the focus. By adjusting the phase of each channel to obtain constructive interference at the bead, the light can be brought to an interferometric focus at its position, thus increasing the bead's fluorescence. To increase the speed of the phase estimation, different methods have been applied, such as a genetic algorithm (GA), spatial frequency modulation and parallel wavefront optimization method [7,8,9]. Fast light modulators, such as the Digital Mircomirror Device (DMD) from Texas Instruments and segmented deformable mirrors from Boston Micromachines, have also been used to further speed up the optimization process [10,11].

In this paper, we propose to use interferometric focusing, rather than conventional geometric focusing, of excitation light onto a guide-star in tissue to increase its fluorescent intensity, thus overcoming signal loss caused by scattering. By minimizing scattering, less power is required to generate a guide-star bright enough for wavefront measurement. With fluorescence from the illuminated laser guide-star, the wavefront can be measured by a Shack-Hartmann wavefront sensor. These measurements will subsequently be used in our AO confocal microscope to overcome refractive image aberrations using adaptive geometric optics. With the interferometric focusing of light, we will increase the illumination of the laser guide-star through scattering tissue by more than two times and potentially double the thickness of tissue that can be corrected using AO microscopy.

2. METHOD

2.1 System layout

Figure 1 shows the configuration of the system. A HeNe laser (LHX1, CVI Melles Griot) with a beam size of 0.65mm was used as the excitation source. The beam was further expanded by lenses L1 and L2, which covers an area with a radius of 4mm on a reflective spatial light modulator (SLM) (LC-R 2500, Holoeye). The excitation light passes through two polarizers, P1 and P2. The former one is used for intensity adjustments and the later one for setting the polarization angle of the incident beam on the SLM. A half-wave plate after the polarizer allows adjusting the polarization angle without changing the intensity of laser. The SLM is located between an analyzer and a half wave plate. The orientations of the half wave plate and analyzer was set so that the SLM operates in a phase-mostly mode. In order to calibrate the SLM input vs. phase relationship, a phase shift interferometer is integrated into the system. The reference mirror is installed on a piezo-actuated nano-positioning stage (17MAX301) in order to introduce a precise phase shift. The reference beam and the measurement beam from the SLM are combined by the beam splitter, so when interference takes place, interference fringes are formed. The interference pattern is projected on a CCD camera by the lens L4. The surface of SLM is conjugate to the front surface of the CCD plane. The phase of the SLM can then be obtained using the Hariharan algorithm and unwrapped by a discrete cosine transformation based on the phase-unwrapping algorithm [12,13]. The calibration system can both register the location of the pupil and be used for displaying the measured wavefront on the SLM. The calibration system can be switched from the main system by a flipper mirror F1.

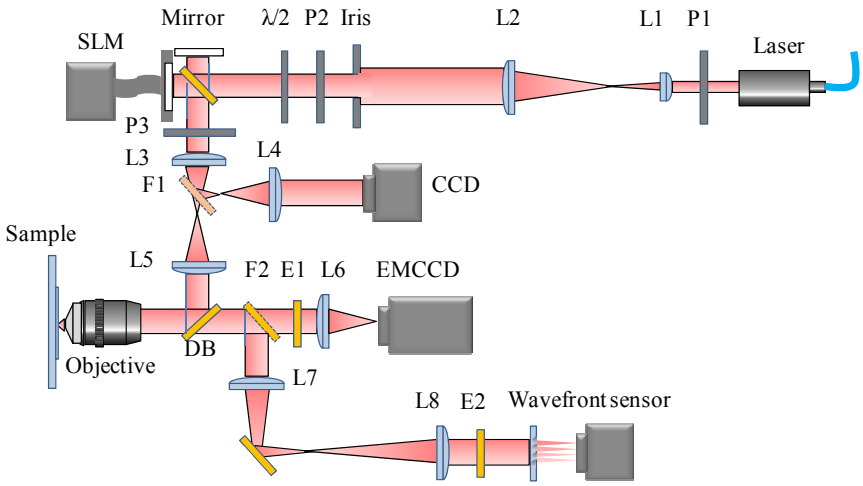

Figure 1. System Layout. L, lens; F, flipper mirror; P, polarizer; DB, dichroic beamplitters; E, emission filter.

The modulated beam is focused on the sample through a 60X water immersion objective with a numerical aperture of 1.1 (Olympus Microscope, Center Valley, PA). Lens L3 and L5 image the exit pupil of the objective on the SLM. The emission light is separated from the excitation light by a dichroic beam splitter DB. After passing through an emission filter, the modulated emission light is finally detected by an electron multiplying CCD (EMCCD) camera (Photometrics) for the estimation of scattering light field phase. After the correct input phase is determined, the position of the flipper mirror (F1) is changed to direct light through a second emission filter (F2) and onto the wavefront sensor, which is composed of a 11×11 element lenslet array (AOA Inc., Cambridge, MA), with a lens diameter of 400 µm, and a focal length of 24 mm (AOA Inc., Cambridge, MA) and a CCD camera (M1400, Dalsa). The pitch of the lenslet array is 400 µm. The sample is installed on a nanopositioning stage (NanoMax, Thorlabs) for precise alignment of the bead. The experimental system was setup on an optical table with vibration isolation as shown in Figure 2.

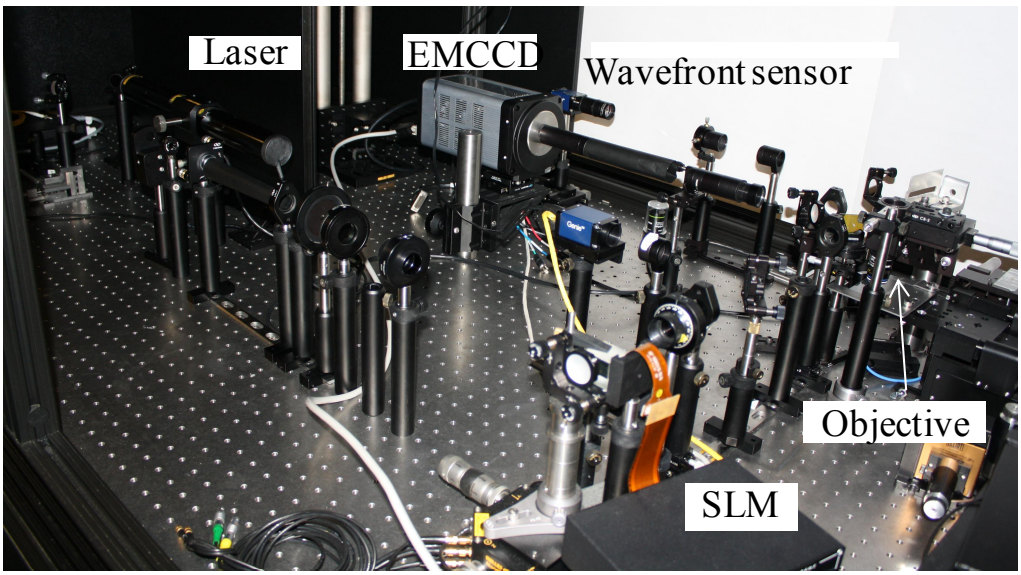

Figure 2. Experimental setup. The system was mounted on an optical table with vibration isolation.

Because the surface of the SLM is not perfectly flat, it leads to optical aberrations in the system. To compensate this system aberration, the phase induced from the SLM's surface is measured using a phase shifting interferometer, which has been integrated into the system. Also an opposite phase map, shown in Figure 3, is applied to the SLM in order to compensate its surface roughness. The spherical aberration induced by the cover glass was initially compensated by adjusting a correction collar on the objective lens.

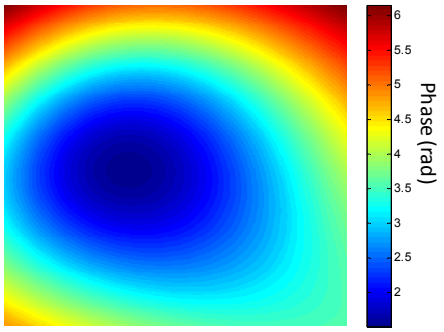

Figure 3. The phase error induced by SLM.

2.2 Interferometric focusing of guide-stars

Imaging of biological tissues often suffers from both aberration in the ballistic light and the scattering affect. The former can be corrected using a deformable mirror. The large iso-planatic angle and high correction speed make it suitable for

live imaging. The accuracy of wavefront measurement depends on the brightness of the guide-star. However, the scattering affect will limit the power of excitation light focused on the guide-star. Increasing the laser power will lead to photobleaching and photodamage of the sample. The background noise further degrades the performance of the wavefront sensor. A promising solution to overcome these issues is interferometric focusing of concentrated light onto guide-stars, such as a fluorescent microsphere or protein. Focusing the light through the tissue without scattering can be achieved when light interferes constructively at the target.

In the proposed system the pupil on the SLM is divided into 316 square segments, which is conjugate to the excitation pupil of the objective. The phase of each segment is modulated independently by the SLM. The emission light from the target is collected by the EMCCD. The sum of the grey values of 20x20 pixels around the target on the image was calculated as the intensity measurement. The step-wise optimization was performed to retrieve the best phase. For each segment, the phase changes from 0 to 2π with 5 steps. The best phase is calculated by fitting intensity measurements for these 5 steps with a sinusoid function. The optimal phase for the current segment is updated before advancing to the next segment. Operation time is mainly limited by the response time of the SLM, which is 80ms in the current setup. The exposure time for EMCCD is set as 20ms. The full correction takes 158s. Increasing the number of segments can improve the correction quality and extend the correction depth, however a longer operation time will expose the sample to potential photobleaching and photodamage.

2.3 Wavefront measurement and correction

The emission light from the guide-stars was detected by a Shack-Hartmann wavefront sensor with a 11x11 lenslet array. It can make a reliable measurement of an aberration up to the first 97 Zernike modes, which is high enough for most biological tissues [14]. Before wavefront measurement, a reference pattern is recorded with a collimated light fed into the system. During measurement, the slope of the wavefront on each sub-aperture was calculated by the displacement of the spot on the wavefront sensor. Then the wavefront is reconstructed by vector-matrix-multiplication (VMM) method [14]. The measurement noise of the wavefront sensor is related to the signal to noise ratio (SNR) of the camera, which can be estimated using [15]:

$$\sigma_m = \sqrt{2}\,\frac{\pi^2 K_g}{4(SNR)}\left[\left(\frac{3}{2}\right)^2 + \left(\frac{\theta d}{\lambda}\right)^2\right] \tag{1}$$

where K_g is a constant to account for centroiding errors due to the fill factor on the CCD, θ is the angular radius of the spot size, λ is the wavelength of the excitation light and d is the sub-aperture diameter. The signal to noise ratio of a detector is given by:

$$SNR = \frac{n_p}{\sqrt{n_p + N_D[n_B^2 + (e/G)^2]}} \tag{2}$$

where n_p is the number of detected photoelectrons per sub-aperture, N_D is the number of detector pixels per sub-aperture. n_B is the number of detected background electrons per pixel, e is the read noise and G is the intensifier gain.

2.4 Sample preparation

Fixed brain slices from an YFP-M line transgenic mouse was prepared. One micron diameter crimson fluorescent microspheres (Invitrogen, Carlsbad, CA) were deposited onto a glass slide and a cover plate for use as laser guide-stars. Sample brain coronal sections at a thickness of 250 μm were cut with a microtome. The tissues are mounted on the microsphere coated glass slide with anti-fade reagents (Invitrogen) and covered with a cover plate.

3. EXPERIMENTAL RESULT

The laser was focused on the microsphere at the bottom of the tissue. The brightest intensity was achieved by precisely adjusting the position of the microsphere in three dimensional space with respect to the objective using a nanopositioning stage. The image of the microsphere is shown in Figure 4(a). Then interferometric focusing was performed to suppress scattering in the sample. A much brighter image is achieved as shown in Figure 4(b). The intensity increases two times. The image from the wavefront sensor before and after interferometric focusing is shown in Figure 4 (c) and (d) respectively. After interferometric focusing, the SNR of the wavefront sensor increased from 64 to 131. RMS error decreases from 0.14λ to 0.07λ. The improvement is more than two times.

Figure 4 (c) and (d) respectively. After interferometric focusing, the SNR of the wavefront sensor increased from 64 to 131. RMS error decreases from 0.14 to 0.07 λ. The improvement is more than two times.

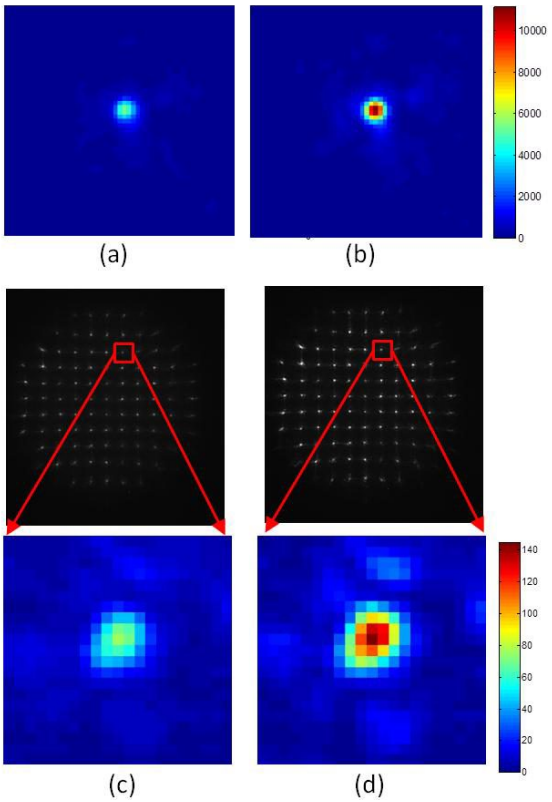

Figure 4. Comparison of result before and after interferometric focusing: images of the microsphere (a) and (b); images from SHWS (c) and (d).

The phase map after optimization is shown in Figure 5 (a). The random phase corresponds to the suppression of the scattering effect from the diffuse light. The donut shape in the phase map is responsible for the wavefront error from the ballistic light. Figure 5 (b) shows the wavefront error measured from the wavefront sensor. The similar shape can be observed on the wavefront. After applying this wavefront measurement to the SLM, the image of the microsphere is shown in Figure 6 (b) and when compared with the image before wavefront correction, Figure 6 (a), the intensity increases 1.5 times.

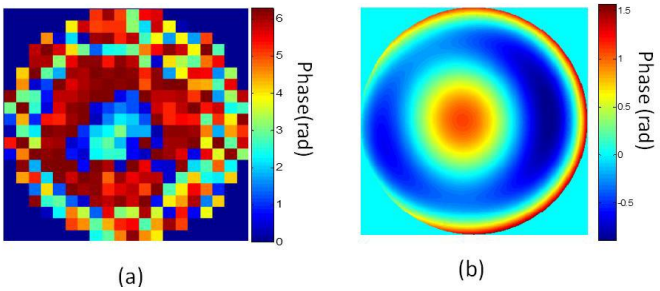

Figure 5. Phase map of the interferometric focusing (a) and wavefront measurement from SHWS (b).

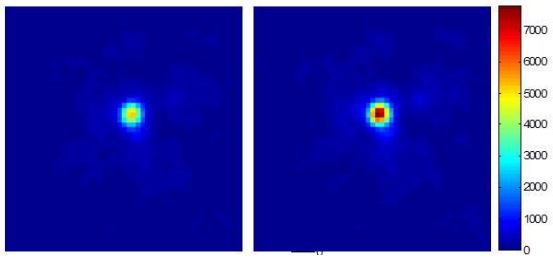

(a) (b)

Figure 6. Images of the microsphere before (a) and after (b) wavefront correction.

4. CONCLUSION

In this paper, we have demonstrated that interferometric focusing, rather than conventional geometric focusing, of excitation light onto a guide-star that is embedded deeply in the tissue, increases its fluorescence intensity. The proposed method can extend the depth of wavefront measurement and correction inside of tissue because of its ability to suppress both scattering of diffused light and aberration of ballistic light. The results show more than two times the improvement in SNR and RMS error of the wavefront measurement. Although only ballistic light in the excitation path is corrected, the intensity after wavefront correction increased by 1.5 times. Because the system setup is only used to verify the proposed wavefront sensing method, only excitation light path was corrected. Further improvements can be achieved if both excitation and emission light paths are corrected.

ACKNOWLEDGMENTS

The results presented herein were obtained at the W.M. Keck Center for Adaptive Optical Microscopy (CfAOM) at University of California Santa Cruz. The CfAOM was made possible by the generous financial support of the W.M. Keck Foundation. We would like to thank Prof. Yi Zuo, MCD Biology, UC Santa Cruz, for the YFP-M line transgenic mouse tissue samples.

REFERENCES

[1] Azucena, O., Crest, J., Kotadia, S., Sullivan, W., Tao, X., Reinig, M., Gavel, D., Olivier, S., and Kubby, J., "Adaptive optics wide-field microscopy using direct wavefront sensing," Optics Letters 36, 825-827 (2011).

[2] Tao, X., Fernandez, B., Azucena, O., Fu, M., Garcia, D., Zuo, Y., Chen, D. C., and Kubby, J., "Adaptive optics confocal microscopy using direct wavefront sensing," Optics Letters 36, 1062-1064 (2011).

[3] Mourant, J. R., Freyer, J. P., Hielscher, A. H., Eick, A. A., Shen, D., and Johnson, T. M., "Mechanisms of Light Scattering from Biological Cells Relevant to Noninvasive Optical-Tissue Diagnostics," Appl. Opt. 37, 3586-3593 (1998) .

[4] Yaqoob, Z., Psaltis, D., Feld, M. S., and Yang, C., "Optical phase conjugation for turbidity suppression in biological samples," Nat. Photonics 2(2), 110–115 (2008).

[5] Xu, X., Liu, H., and Wang, L. V., "Time-reversed ultrasonically encoded optical focusing into scattering media," Nat. Photonics 5(3), 154–157 (2011).

[6] Vellekoop, I. M., van Putten, E. G., Lagendijk, A., and Mosk, A. P., "Demixing light paths inside disordered metamaterials," Opt. Express 16, 67-80 (2008) .

[7] Conkey, D. B., Brown, A. N., Caravaca-Aguirre, A. M., and Piestun, R., "Genetic algorithm optimization for focusing through turbid media in noisy environments," Opt. Express 20, 4840-4849 (2012).

[8] Cui, M., "A high speed wavefront determination method based on spatial frequency modulations for focusing light through random scattering media," Opt. Express 19, 2989-2995 (2011) .

[9] Fiolka, R., Si, K., and Cui, M., "Parallel wavefront measurements in ultrasound pulse guided digital phase conjugation," Opt. Express 20, 24827-24834 (2012).

[10] Conkey, D. B., Caravaca-Aguirre, A. M., and Piestun, R., "High-speed scattering medium characterization with application to focusing light through turbid media," Opt. Express 20, 1733-1740 (2012).
[11] Stockbridge, C., Lu, Y., Moore, J., Hoffman, S., Paxman, R., Toussaint, K., and Bifano, T., "Focusing through dynamic scattering media," Optics Express 20, 15086-15092 (2012).
[12] Malacara, D., [Optical Shop Testing], Wiley, New York, (2007).
[13] Schofield, M. A., and Zhu, Y., "Fast phase unwrapping algorithm for interferometric applications," Opt. Lett. 28, 1194-1196 (2003).
[14] Porter, J., Queener, H., Lin, J., Thorn, K., and Awwal, A. A. S., [Adaptive Optics for Vision Science: Principles, Practices, Design and Applications], Wiley, (2006).
[15] Hardy, J. W., [Adaptive Optics for Astronomical Telescopes], Oxford University Press, (1998).